2011년 8월

석사학위논문

컬러센서를 이용한 조명 및 컬러분포 측정장치 개발

Development of an Illumination Measurement Device for Color Distribution Based on a CIE 1931 Sensor

조선대학교 대학원

전자공학과

도키손

컬러센서를 이용한 조명 및 컬러분포 측정장치 개발

Development of an Illumination Measurement Device for Color Distribution Based on a CIE 1931 Sensor

2011년 8 월 25 일

조선대학교 대학원

전자공학과

도키손

컬러센서를 이용한 조명 및 컬러분포 측정장치 개발

지도교수 이 충 규

이 논문을 전자공학 석사학위신청 논문으로 제출함

2011년 4월

조선대학교 대학원

전자공학과

도키손

도키손의 석사학위논문을 인준함

위원장 조선대학교 조교수 김주형 (인)

위원 조선대학교 조교수 강문수 (인)

위원 조선대학교 조교수 이충규 (인)

2011년 5 월 일

조선대학교 대학원

Contents

List of Figure

List of Table

초 록

컬러센서를 이용한 조명 및 컬러분포 측정장치 개발

도 키 손

지도교수 : 이 충 규

조선대학교일반대학원전자공학과

LED 는 저전력 소자이고 수명이 길며 밝은 광도 및 다양한 컬러를 제공할 수 있기 때문에, 최근 조명용 소자로서 활발한 연구개발이 수행되고 있다. 이러한 장점을 구비한 LED 를 사용함으로써, 사람들은 전력 및 에너지에 관한 많은 문제를 해결할 수 있을 것으로 기대하며, 다양한 응용분야에 적용이 시도되고 있다. 따라서, 점광원 특성을 갖는 조명용 LED 로부터 방출된 광도 또는 컬러 분포특성을 측정하기 위한 장치를 개발할 필요성이 대두되었다.

본 논문에서는 조명산업에서 각광받는 소자인 LED 의 컬러 분포가 어떻게 되어있는지 측정하기 위해, 컬러센서를 기반으로 하여 조명 및 컬러 분포측정이 가능한 측정장치를 개발하기 위한 연구를 기술한다. 특히, 수많은 색상 중에 빨강, 파랑, 녹색 성분의 빛만 추출한 후 CIE 1931 에 따라 그 상대적인 비율을 통해 분포특성을 연구한다.

본 연구를 통해 개발된 조명 및 컬러분포 측정장치는 배열형 센서 모듈과 배열형 센서모듈로부터 신호를 효율적으로 측정하기 위한 제어모듈 그리고 측정신호를 적절히 사용자에게 제공하기 위한 PC 인터페이스로 구성되어 있다.

배열형 센서 모듈은 데이터 처리와 측정을 위해 컨트롤러 안에 CIE1931 컬러센서와 ARM 프로세서 툴에 기반한 96 MHz 마이크로컨트롤러로 설계된다. 배열형 센서모듈은 16x4 배열 안에 64 개의 컬러센서를 포함한다. 또한, 매우 약한 빛도 감지할 수 있도록 설계된다. 측정된 데이터 신호들은 USB 2.0 을 통해 변환되어 PC 스크린을 통해 실시간 컬러본포 측정이 가능하다. 이 컬러분포 측정장치를 통하여 조명 빛 안에 있는 빨강, 파랑, 녹색 성분의 빛을 측정할 수 있고 각각 세 가지 빛을 성분별로 실시간 모니터링 할 수 있다.

따라서, 측정장치는 LED 를 사용한 조명장치를 위해 컬러 분포측정을 통한 성능 검증 및 설계과정에 중요한 역할을 할 수 있을 것으로 기대한다.

ABSTRACT

Development of an Illumination Measurement Device for Color Distribution Based on a CIE 1931 Sensor

Do Ky Son

Advisor: Prof. Lee Chung Ghiu, Ph.D.

Department of Electronic Engineering,

Graduate School of Chosun University.

In this thesis, an easy-to-use measurement device for illumination distribution is developed. The device consists of a sensor array module, a control module, and a PC interface. The sensor array module incorporates CIE 1931 color sensors and the ARM-based 96 MHz microcontroller in the controller for measurement and data processing. The sensor array module contains 64 color sensors arranged in a 16×4 array. The sensitivity of the sensor array module can be adjusted to measure a weak light. The measurement data and control signals are exchanged via USB 2.0 standard. Using the measurement device, the illumination distribution is measured for colors of red, green, and blue and is graphically determined. The device can be used for the measurement of illumination distribution, the design, and the adjustment of LED illumination.

Chapter 1

INTRODUCTION

Nowadays, many visible spectrum light-emitting diodes (LEDs) are actively being developed and their basic optical and electrical characteristics are well described in [1]. Due to the commercial potential of LEDs with visible light emission, LED illumination draws a great deal of attention from LED manufacturers, LED driving IC manufacturers, LED backlight unit (BLU) manufacturers, illumination designers, and architects seeking new forms of illumination. LED illumination offers the user numerous advantages, including considerable power reduction, extreme durability, size reduction, a wide color gamut, improved degree of freedom for the illumination shape, and a high resistance to shock and vibration.

Furthermore, LED illumination costs less to maintain due to its long lifetime and the fact that the price for the chips per unit of luminous flux is decreasing [2]. As a result, the LED with visible light emission is very useful not only for illumination and LED BLU, but also for the environment and for indoor decorations and advertisements. Therefore, colorful LEDs will be a versatile light source for all those applications. From the illumination point of view, the visible (red, green, blue) LEDs are used to form illumination devices and colorful displays [3]. The driving current for each LED can be controlled quickly and independently with appropriate driving circuitry to maintain its brightness and color [4], [5]. These two characteristics makes a visible LED be a prominent candidate for lighting instruments. In such a case, it is necessary to measure illuminance to ensure that an LED lamp provides an illumination level of 300 – 1500 lx, based on the ISO standard for office work [6].

Since LED lighting is composed of individual LEDs, the illumination on a target surface is patterned, depending upon the density of the LEDs, the LED directionality, the shape of an LED array, etc. Therefore, the measurement of illumination distribution is substantial for the design and characterization of LED illumination. Specifically, to analyze the irradiance

performances from the LED arrays, the design expressions for illumination uniformity in a near-target plane from LED arrays have been derived [7], and the far-field condition for an array of LEDs is analyzed by LED radiation pattern, array geometry, and the number of LEDs [8]. Moreover, to achieve uniform illumination, a design process using a surface-tailored lens has been proposed [9] and an efficient coupler design has been reported [10].

Except for precise measurement in laboratory experiment or an exact calibration process, the LED is supposed to sufficiently ensure that human eyes perceive that the brightness and color are evenly distributed or the chromaticity of certain measurement points is well distributed. A certain color measurement needs multi-point calibration with a calibrating procedure [11] and a simultaneous color measurement, and white balancing for RGB white LEDs, was demonstrated by using a buried double p-n junction (BDJ) photo detector, which was fabricated by the same authors [12]. A chromatic property measurement system for LED was developed based on the spectroradiometric method using a photomultiplier [13]. These are not easy-to-use simple measurement devices for LED applications. Furthermore, a hand-held illuminance measurement system with versatile functions [14] is available. To measure multiple points simultaneously, the device needs to connect multiple remote detector heads. Therefore, easy-to-use and fast illumination measurement devices would be useful without a complex measurement process, such as in a precise measurement or an exact calibration process.

In this thesis, I report a device for easy-to-use illumination measurement using a color sensor array. The color sensor is in an integrated circuit (IC) and is equipped with an XYZ tri-stimulus function, based on the known observer function CIE 1931 [15]. Each sensor has a tolerance of nearly 1 % variation of wavelength. The sensor array module with an appropriate control circuit makes it easy to measure and analyze the illumination and color distributions over a two-dimensional surface at one time. Each sensor in the array module can measure a true color, based on three independent CIE 1931 color matching functions: $\bar{x}$, $\bar{y}$, and $\bar{z}$ [16]. The analog signal from each sensor module is converted to a digital signal. The measurement device provides the illumination and color distributions over the surface.

1.1 Thesis objectives

In this thesis, I report a device for easy-to-use illumination measurement using a color sensor array. We could use it to detect the distributions of brightness and colors for a certain illumination environment. When the LED illumination is widely used in the near future, the device is expected to be used as a useful tool for illumination distribution or LED illumination system.

By using true color sensor and ARM microcontroller this device have many advantages:

- Easy to use.
- Fast measurement.
- Without complex and cheap.

1.2 Thesis organization

The paper is organized as follows. Section 2 describes the configuration of the developed measurement device, including the component descriptions. Measurement and performance using the device are described in Section 3. Section 4 deals with the discussions on future development. The paper is concluded with Section 5.

Chapter 2

PHOTOMETRY

2.1 CIE 1931 color space standard

In the study of color perception, one of the first mathematically defined color spaces was the **CIE 1931 XYZ color space**, created by the International Commission on Illumination (CIE) in 1931.

The CIE XYZ color space was derived from a series of experiments done in the late 1920s by W. David Wright and John Guild. Their experimental results were combined into the specification of the CIE RGB color space, from which the CIE XYZ color space was derived. This article is concerned with both of these color spaces.

Tristimulus values

The human eye has photoreceptors (called cone cells) for medium- and high-brightness color vision, with sensitivity peaks in short (*S*, 420–440 nm), middle (*M*, 530–540 nm), and long (*L*, 560–580 nm) wavelengths (there is also the low-brightness monochromatic "night-vision" receptor, called rod cell, with peak sensitivity at 490-495 nm). Thus, in principle, three parameters describe a color sensation. The **tristimulus values** of a color are the amounts of three primary colors in a three-component additive color model needed to match that test color. The tristimulus values are most often given in the CIE 1931 color space, in which they are denoted *X*, *Y*, and *Z*.

Any specific method for associating tristimulus values with each color is called a color space. CIE XYZ, one of many such spaces, is a commonly used standard, and serves as the basis from which many other color spaces are defined.

The CIE standard observer

In the CIE XYZ color space, the tristimulus values are not the *S*, *M*, and *L* responses of the human eye, but rather a set of tristimulus values called *X*, *Y*, and *Z*, which are roughly red, green and blue, respectively (note that the X,Y,Z values are not physically observed red, green, blue colors. Rather, they may be thought of as 'derived' parameters from the red, green, blue colors). Two light sources, made up of different mixtures of various wavelengths, may appear to be the same color; this effect is called metamerism. Two light sources have the same apparent color to an observer when they have the same tristimulus values, no matter what spectral distributions of light were used to produce them.

Due to the nature of the distribution of cones in the eye, the tristimulus values depend on the observer's field of view. To eliminate this variable, the CIE defined the **standard (colorimetric) observer**. Originally this was taken to be the chromatic response of the average human viewing through a 2° angle, due to the belief that the color-sensitive cones resided within a 2° arc of the fovea. Thus the *CIE 1931 Standard Observer* is also known as the *CIE 1931 2° Standard Observer*. A more modern but less-used alternative is the *CIE 1964 10° Standard Observer*, which is derived from the work of Stiles and Burch, and Speranskaya.

For the 10° experiments, the observers were instructed to ignore the central 2° spot. The 1964 Supplementary Standard Observer is recommended for more than about a 4° field of view. Both standard observers are discredited at 5 nm wavelength intervals and distributed by the CIE. The standard observer is characterized by three *color matching functions*. The derivation of the CIE standard observer from color matching experiments is given below, after the description of the CIE RGB space.

Color matching functions

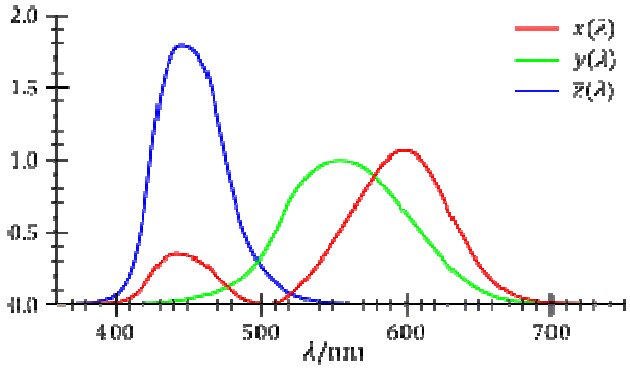

Fig 2.1 The CIE standard observer color matching functions

The **color matching functions** are the numerical description of the chromatic response of the *observer* (described above).

The CIE has defined a set of three *color-matching functions*, called $\bar{x}(\lambda)$, $\bar{y}(\lambda)$, and $\bar{z}(\lambda)$ which can be thought of as the spectral sensitivity curves of three linear light detectors that yield the CIE XYZ tristimulus values *X*, *Y*, and *Z*. The tabulated numerical values of these functions are known collectively as the CIE standard observer.

The tristimulus values for a color with a spectral power distribution $I(\lambda)$ are given in terms of the standard observer by:

$$X = \int_0^\infty I(\lambda)\bar{x}(\lambda)d\lambda\,, \tag{1}$$

$$Y = \int_0^\infty I(\lambda)\bar{y}(\lambda)d\lambda\,, \tag{2}$$

$$Z = \int_0^\infty I(\lambda)\bar{z}(\lambda)d\lambda\,, \tag{3}$$

Where λ is the wavelength of the equivalent monochromatic light (measured in nanometers).

Other observers, such as for the CIE RGB space or other RGB color spaces, are defined by other sets of three color-matching functions, and lead to tristimulus values in those other spaces.

The values of X, Y, and Z are bounded if the intensity spectrum $I(\lambda)$ is bounded.

The CIE *xy* chromaticity diagram and the CIE *xyY* color space

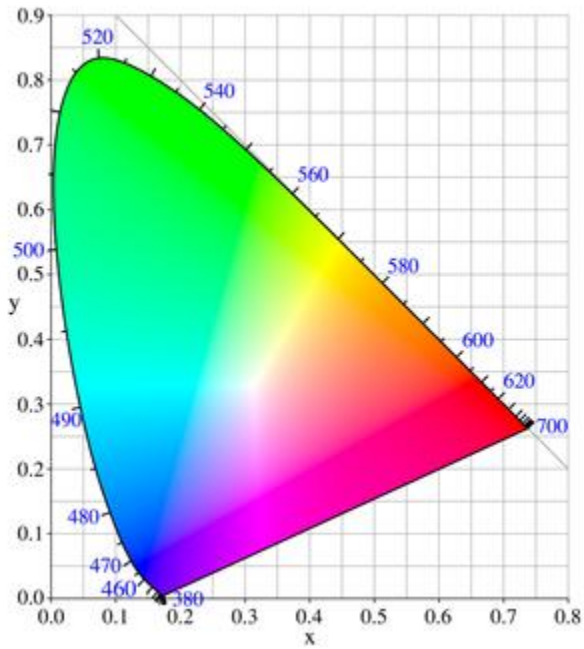

Fig 2.2 The CIE 1931 color space chromaticity diagram.

The outer curved boundary is the spectral (or monochromatic) locus, with wavelengths shown in nanometers. Note that the image itself describes colors usingsRGB and colors outside the sRGB gamut cannot be displayed properly. Depending on the color space and calibration of your display device, the sRGB colors may not be displayed properly either. This diagram displays the maximallly saturated bright colors that can be produced by a computer monitor or television set.

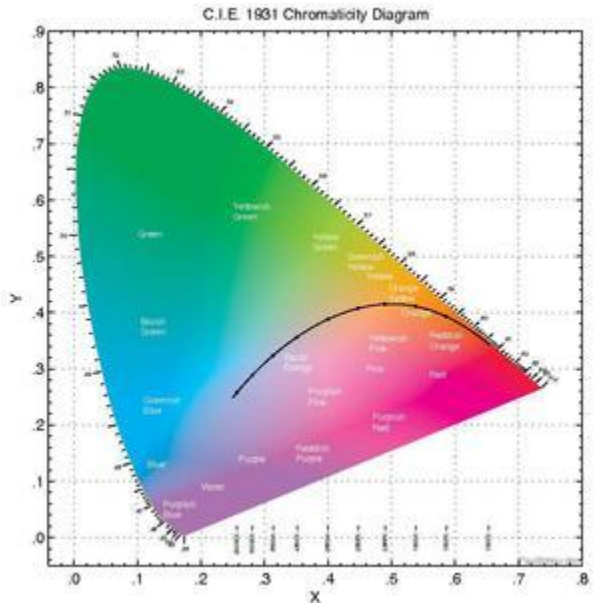

Fig 2.3 The CIE 1931 color space chromaticity diagram rendered

The CIE 1931 color space chromaticity diagram rendered in terms of the colors of lower saturation and value than those displayed in the diagram above that can be produced by pigments, such as those used in printing. The color names are from the Munsell color system.

Since the human eye has three types of color sensors that respond to different ranges of wavelengths, a full plot of all visible colors is a three-dimensional figure. However, the concept of color can be divided into two parts: brightness and chromaticity. For example, the color white is a bright color, while the color grey is considered to be a less bright version of that same white. In other words, the chromaticity of white and grey are the same while their brightness differs.

The CIE XYZ color space was deliberately designed so that the *Y* parameter was a measure of the brightness or luminance of a color. The chromaticity of a color was then specified by the two derived parameters *x* and *y*, two of the three normalized values which are functions of all three tristimulus values *X*, *Y*, and *Z*:

$$x = \frac{X}{X + Y + Z}$$

$$y = \frac{Y}{X + Y + Z}$$

$$z = \frac{Z}{X + Y + Z}$$

The derived color space specified by x, y, and Y is known as the **CIE xyY** color space and is widely used to specify colors in practice.

The *X* and *Z* tristimulus values can be calculated back from the chromaticity values *x* and *y* and the *Y* tristimulus value:

$$X = \frac{Y}{y} x$$

$$Z = \frac{Y}{y}(1 - x - y)$$

The figure on the right shows the related chromaticity diagram. The outer curved boundary is the *spectral locus*, with wavelengths shown in nanometers. Note that the chromaticity diagram is a tool to specify how the human eye will experience light with a given spectrum. It cannot specify colors of objects (or printing inks), since the chromaticity observed while looking at an object depends on the light source as well.

Mathematically, *x* and *y* are projective coordinates and the colors of the chromaticity diagram occupy a region of the real projective plane.

The chromaticity diagram illustrates a number of interesting properties of the CIE XYZ color space:

- The diagram represents all of the chromaticities visible to the average person. These are shown in color and this region is called the gamut of human vision. The gamut of all visible chromaticities on the CIE plot is the tongue-shaped or horseshoe-shaped figure shown in color. The curved edge of the gamut is called the *spectral locus* and

corresponds to monochromatic light, with wavelengths listed in nanometers. The straight edge on the lower part of the gamut is called the line of purples. These colors, although they are on the border of the gamut, have no counterpart in monochromatic light. Less saturated colors appear in the interior of the figure with white at the center.

- It is seen that all visible chromaticities correspond to non-negative values of x, y, and z (and therefore to non-negative values of X, Y, and Z).

- If one chooses any two points of color on the chromaticity diagram, then all the colors that lie in a straight line between the two points can be formed by mixing these two colors. It follows that the gamut of colors must be convex in shape. All colors that can be formed by mixing three sources are found inside the triangle formed by the source points on the chromaticity diagram (and so on for multiple sources).

- An equal mixture of two equally bright colors will not generally lie on the midpoint of that line segment. In more general terms, a distance on the xy chromaticity diagram does not correspond to the degree of difference between two colors. In the early 1940s, David MacAdam studied the nature of visual sensitivity to color differences, and summarized his results in the concept of a MacAdam ellipse. Based on the work of MacAdam, the CIE 1960, CIE 1964, and CIE 1976 color spaces were developed, with the goal of achieving perceptual uniformity (have an equal distance in the color space correspond to equal differences in color). Although they were a distinct improvement over the CIE 1931 system, they were not completely free of distortion.

- It can be seen that, given three real sources, these sources cannot cover the gamut of human vision. Geometrically stated, there are no three points within the gamut that form a triangle that includes the entire gamut; or more simply, the gamut of human vision is not a triangle.

- Light with a flat power spectrum in terms of wavelength (equal power in every 1 nm interval) corresponds to the point $(x,y) = (1/3,1/3)$.

2.2 Color sensor

The MTCS - TIAM2 from MAZet Company was used to sense color. MTCS – TIAM2 is a high integrated True Color Sensor IC with integrated transimpedance amplifier in a small plastic package on a PCB-carrier. It includes the standard XYZ (RGB) filters based on the known observer function CIE 1931. So the sensor is specialized for fast and absolute, high accuracy color measurement.

The True Color Sensors are made of 19 x 3 photo diodes (special PIN silicon technology with blue-enhanced) integrated on chip. The diodes are carried out as segments of a multiple-element hexagonal matrix structure with the diameter of 2.0 mm. The technology Si-PIN photo diodes allow signal frequencies up to high-range. In order to achieve a small cross talk between the colored photodiodes the individual sectors were separated from each other by additional structures – separate diode. The photodiodes are sensitized on chip with high-quality and long-time stabile dielectric spectral filters (named True Color Filter). These filters correspond to the primary color standard CIE 1931(Commission Internationale de l'Eclairage or International Commission on Illumination) and/or the German standard DIN 5033.

Fig 2.4 True color sensor.

- High-resolution conversion of colored light to voltages.

- Simultaneous measurement of XYZ three colors.
- High sensitiveness, transmission, signal frequency.
- No ageing of the filter, high temperature stability.
- Reduced cross talk and linear amplifying.

- Programmable adjustment of transimpedance.
- Power down feature.
- Small in size, lead free.
- Alike tri-stimulus interference filter for color measurement to DIN 5033 (CIE 1931).
- LCC package (SMD).

EU RoHS-compliant2.

Chapter 3

DEVICE CONFIGURATION

3.1 Device organization

Figure 1 show the organization of the measurement device, which consists of three parts. The sensor array module includes a two-dimensional color sensor array, multiplexers, and an analog-to-digital converter. The control module consists of a microcontroller, a power supply, and various connectors. The other part provides the interface between the control module and the PC.

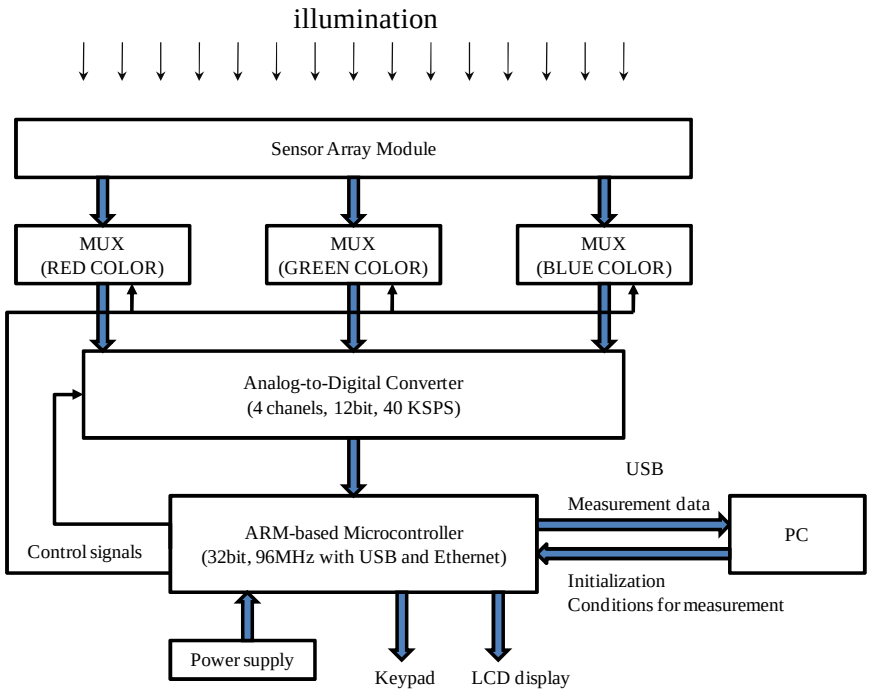

Fig 3.1 Block diagram of the measurement device.

The color sensor array is composed of 64 color sensors in a 16 × 4 array. Each sensor includes the standard XYZ (RGB) filters based on the known observer function CIE 1931 [16]. The photocurrent from a color sensor is converted into the voltage inside the color sensor IC, which stands for direct coordinates for the standard 1931 color space. The output voltage signals from the sensor array module are then multiplexed and converted into digital signals. Compact and portable, the sensor array module is suitable for hand-held applications. Using the two dimensional array of color sensors, fast and absolute color measurement over a surface is possible.

The analog signals containing illumination and color information from 64 sensors are collected by multiplexers, and the ARM-based microcontroller in the control module processes digital signals and sends them to the PC through the USB 2.0 interface. The measurement data fed into the PC is processed to draw a two-dimensional figure for illumination and color distribution, which are described in Section 3. The LCD display in the control module shows the status of the measurement device and the basic parameters for measurement are set by using four keypads.

3.2 Multiplexer and analog-to-digital conversion

A monolithic CMOS dual 16-channel analog multiplexer (ADG726, Analog Devices) switches one of 16 inputs, as determined by the 4-bit binary address lines A0, A1, A2, and A3. With this multiplexing capability, simultaneous measurement from 64 color sensors is possible. The multiplexer works well with a 1.8 V to 5.5 V single supply or a 2.5 V dual supply. It has only 4 Ω resistance and needs only 30 ns for switching. Therefore, it provides the number of address lines and sufficient switching time to ensure accuracy and speed for this development.

The analog-to-digital converter (ADS7824, Burr-Brown Company) is used to convert the analog signal from the sensor array module to a digital signal. The converted digital signal is a 12-bit data stream, which consumes only 50 mW at its maximum. Laser-trimmed scaling resistors provide the standard industrial ±10V input range and the channel-to-channel matching of ±0.1%.

Figure 3 shows the block diagram for connectivity between the multiplexer and the analog-to-digital converter (ADC). The multiplexing of 64 sensors needs 192 color signal lines. However, we use only one ADC with four inputs by using the multiplexers to collect the signals from 64 sensors. The microcontroller controls the multiplexer and chooses which of the signal lines is to be connected to the ADC. The signal conversion processes from multiplexing to ADC are summarized into the following three steps: 1) choose a specific signal line using a 5 bits address, 2) convert the analog signal to a digital signal, and 3) obtain the digital values.

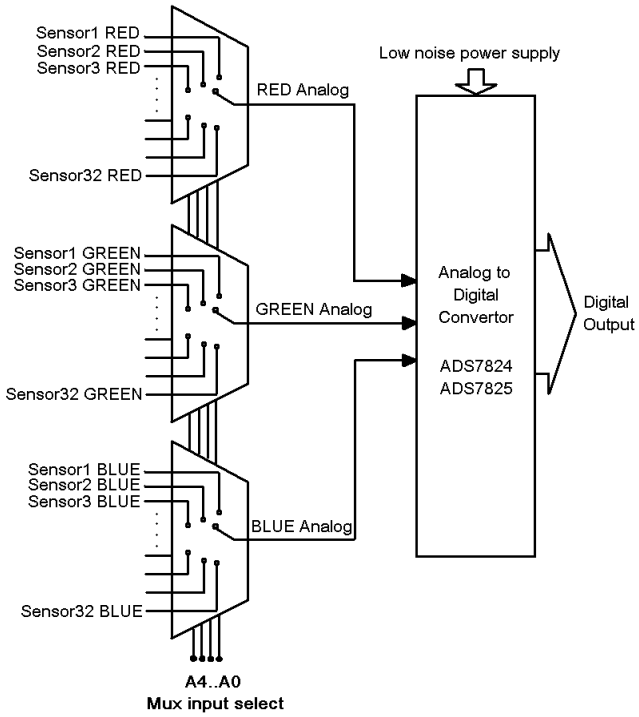

Fig 3.2 Block diagram for connectivity between multiplexing and analog-to-digital conversion. Analog signals are multiplexed and converted into digital signals.

3.3 ARM-based microcontroller

The microcontroller used for this development is an ARM-based microcontroller (STR912FAW46X6, ST Microelectronics). This microcontroller is a32-bit ARM (advanced RISC machine) device. The general information on ARM processors is found in [18]. The

microcontroller is a 96 MHz ARM based microcontroller unit (MCU) with an ARM966E-S RISC core. It has Harvard architecture, a 5-stage pipeline, and tightly-coupled memories (SRAM and flash). The microcontroller also has dual burst flash memories, 32-bits wide with a 1 MB main flash memory, and a 128 KB secondary flash memory. Furthermore, it supports 10 communication interfaces, including 10/100 Ethernet MAC with DMA (direct memory access) and MII (medium independent interface) [19], as well as a USB full-speed (12 Mbps) slave device [20]. By using the microcontroller with USB full-speed support, we can ensure the data transmission speed of the measurement device.

3.4 Printed circuit boards

The printed circuit boards (PCBs) are developed in a DXP 2004 Altium environment and are shown in Fig. 4-5. We adopted 4-layer PCBs. Each PCB has a ground layer and its surface layers for wiring are covered with ground areas to reduce the noise from the outside of the PCB.

The device includes two modules: a control module and a sensor array module. Figure 4 shows the control module with the microcontroller, the Ethernet connector, the USB connector, the power supply unit, the LCD connector, the push button, the sensor connector, and the JTAG connector.

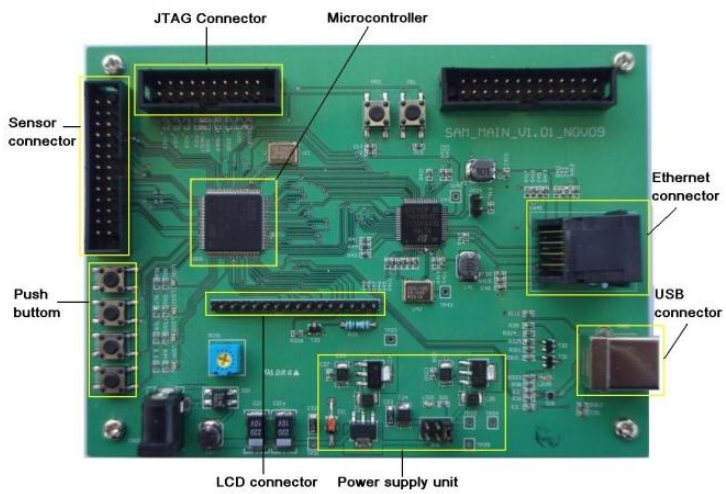

Fig 3.3 Printed circuit board of the control module.

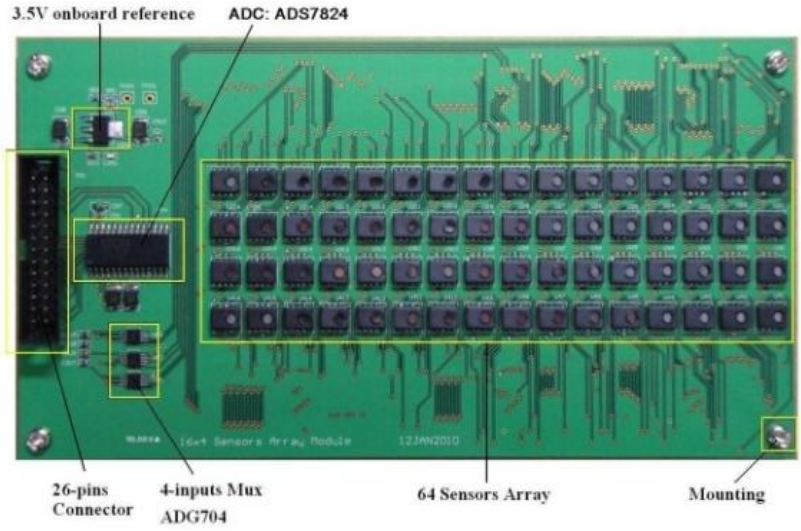

(a) front side

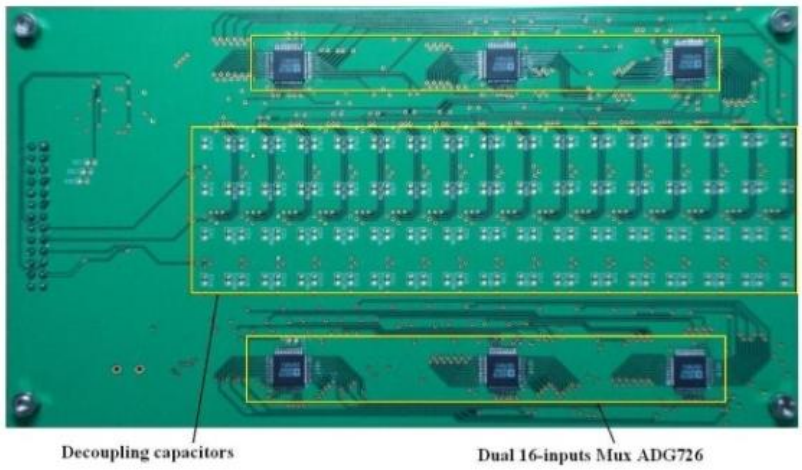

(b) back side

Fig 3.4 Printed circuit board of the sensor array module; (a) front side, and (b) back side.

The top and bottom photos of the sensor array module are shown in Fig. 5. This module includes the 16x4 sensor array and the ADC (ADS7824), with a 3.5 V onboard reference and

the 4-input multiplexers (ADG704) with a 26-pin connector. The bottom contains dual 16-input multiplexers (ADG726) and decoupling capacitors.

3.5 USB interface

The USB driver was developed based on a virtual instrument standard architecture (VISA) tool in LabVIEW [21]. After setting up the developed driver and connecting the control module to the PC, the module becomes a USB device as shown in Fig. 6.

Fig 3.5 Screenshot of USB driver initialization in the PC operating system.

Table 1 shows the frame format for the data packet between the PC and the control module. The frame packet from the PC to the control module begins with a 1 byte Device ID, a 1 byte Command ID, and 8 bytes data, successively, and is finished with a 1 byte checksum CRC (cyclic redundancy code). The frame packet from the control module to the PC begins with a 1 byte Sensor ID, then a 1 byte Color ID, and 32 bytes data, successively, and is finished with a 1 by checksum CRC.

(a)

Device ID	Command ID	Byte1	…	Byte8	CRC

(b)

Sensor ID	Color ID	Byte1	…	Byte32	CRC

Table 1 (*a) Frame Packet from PC to Control Module; (b) Frame Packet from Control Module to PC*

3.6 Labview interface

Front panel interface

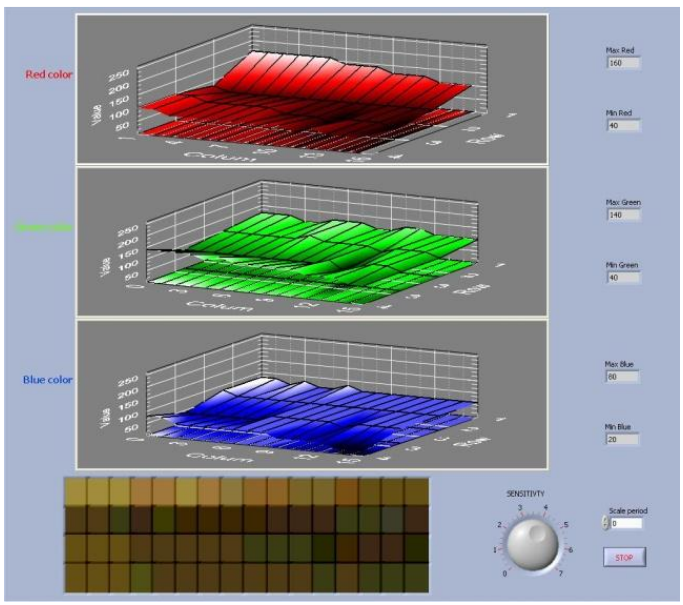

Fig 3.6 Labview front panel interface

On the front panel we have 3 3D graphs that show The Red, Green, Blue values of 64 sensors. The true color was showed on the picture in the bottom of frond panel. We can use the knob to change value of sensor's sensitivity from 0 to 7. Sensor is max sensitive if the sensitivity value is 7. 6 value indicators show the maximum and minimum value of red, green and blue colors. When Labview is running, we can stop by using Stop button.

Block diagram

By following this chart I made a program to show the measurement result on Labview front panel.

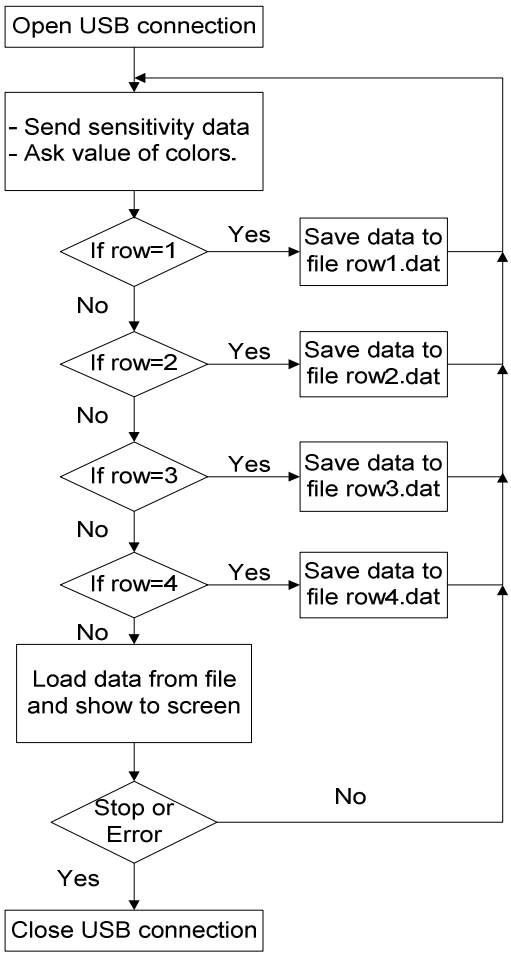

Fig 3.7 Labview follow chart

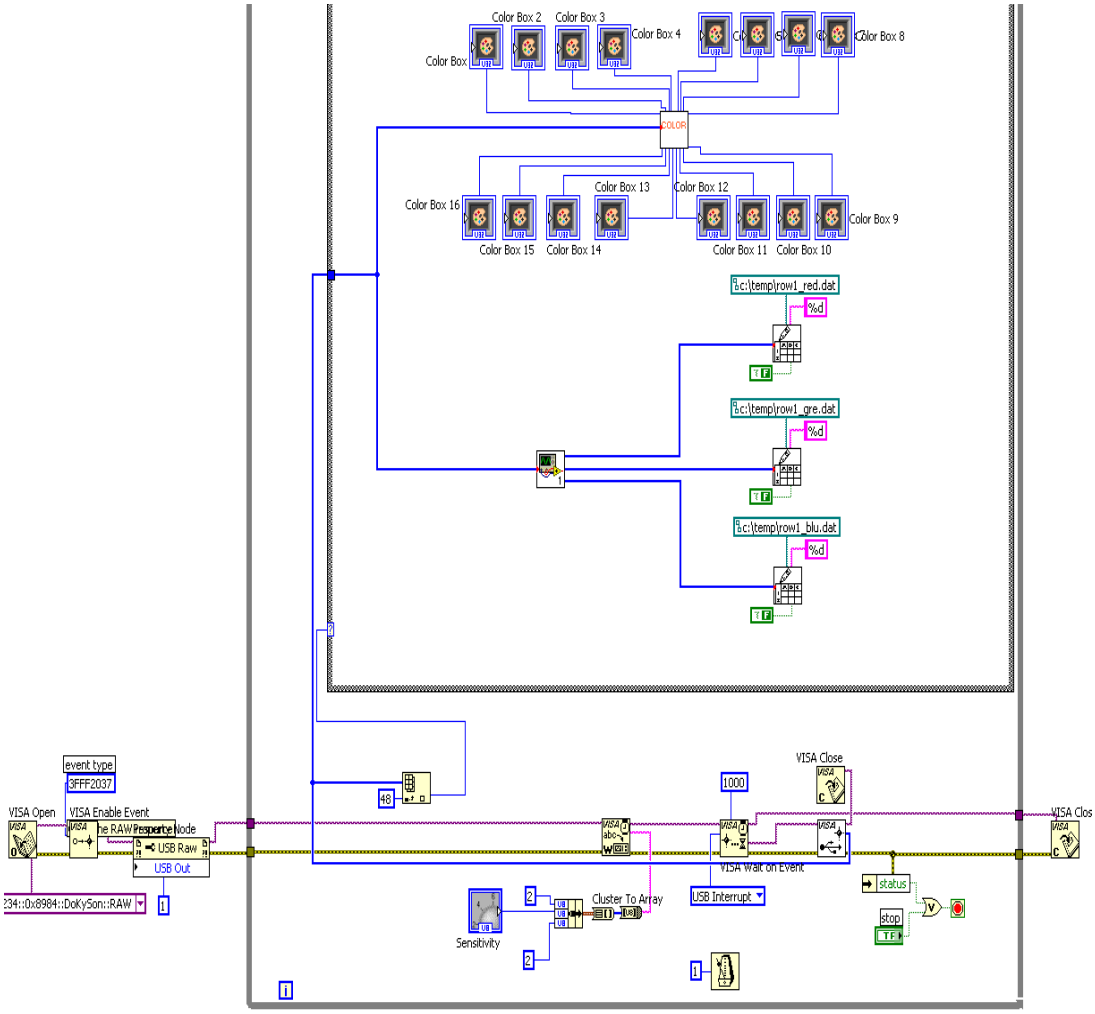

Fig 3.7 Labview block diagram

Block diagram detail

VISA open function:

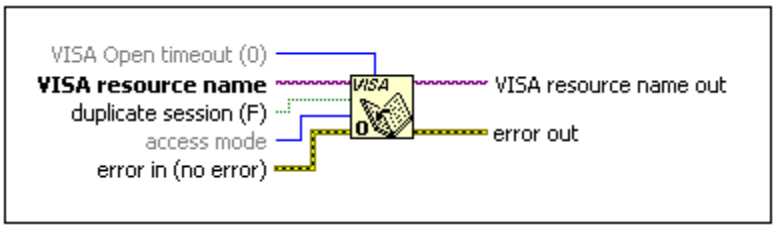

Fig 3.8 VISA open function in Labview.

VISA Open timeout specifies the maximum time period, in milliseconds, that VISA Open waits before returning an error. It does not set the I/O timeout. To specify the timeout used for future operations on the VISA session, use VISA Set Timeout.
VISA resource name specifies the resource to be opened. This control also specifies the session and class.
If **duplicate session** is TRUE and there is currently a session opened to the resource, another session is opened to the resource. If **duplicate session** is set to FALSE and a session is opened to the resource, the open session is used. A VISA session is a unique logical identifier used by VISA to communicate with a resource.
Access mode specifies how to access the device. This input accepts the following values.
Error in describes error conditions that occur before this VI or function runs. The default is no error. If an error occurred before this VI or function runs, the VI or function passes the **error in** value to **error out**. This VI or function runs normally only if no error occurred before this VI or function runs. If an error occurs while this VI or function runs, it runs normally and sets its own error status in **error out**.
VISA resource name out is the resource to which a VISA session is opened and its class. The class matches that of the **VISA resource name** input.
Error out contains error information. If **error in** indicates that an error occurred before this VI or function ran, **error out** contains the same error information. Otherwise, it describes the error status that this VI or function produces.

VISA write function:

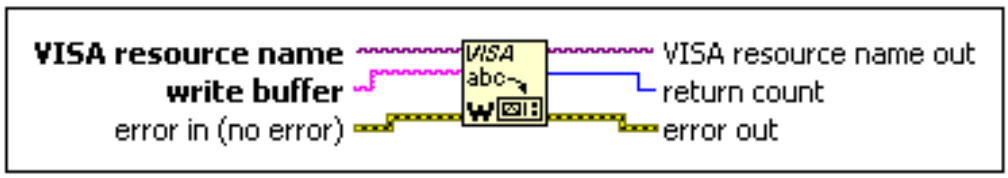

Fig 3.9 VISA write function in Labview.

VISA resource name specifies the resource to be opened. This control also specifies the session and class. Refer to VISA Resource Name Control for more information.
Write buffer contains the data to be written to the device.
Error in describes error conditions that occur before this VI or function runs. The default is no error. If an error occurred before this VI or function runs, the VI or function passes the **error in** value to **error out**. This VI or function runs normally only if no error occurred before this VI or function runs. If an error occurs while this VI or function runs, it runs normally and sets its own error status in **error out**.

VISA resource name out is a copy of the **VISA resource name** that VISA functions return.
Return Count contains the actual number of bytes written.
Error out contains error information. If **error in** indicates that an error occurred before this VI or function ran, **error out** contains the same error information. Otherwise, it describes the error status that this VI or function produces.

VISA Wait on Event Function:

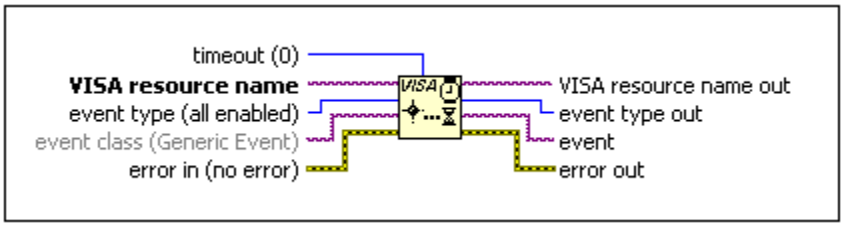

Fig 2.10 VISA Wait on Event function in Labview.

Timeout is the period of time in milliseconds to wait for the event.
VISA resource name specifies the resource to be opened. This control also specifies the session and class.
Event type is the logical event identifier. You can select from the following VISA event types.
Event class specifies the class of event for which the function waits. The default is Generic Event, meaning the function recognizes any class of event.
Error in describes error conditions that occur before this VI or function runs. The default is no error. If an error occurred before this VI or function runs, the VI or function passes the **error in** value to **error out**.
VISA resource name out is a copy of the **VISA resource name** that VISA functions return.
Event type out identifies the event type received if the wait was successful.
Event is valid if the wait was successful. Wire **event** to a Property Node to get further information about the event. Wire **event** to the VISA Close function when examination of the event is complete.
Error out contains error information. If **error in** indicates that an error occurred before this VI or function ran, **error out** contains the same error information. Otherwise, it describes the error status that this VI or function produces.

VISA Get USB Interrupt Data VI:

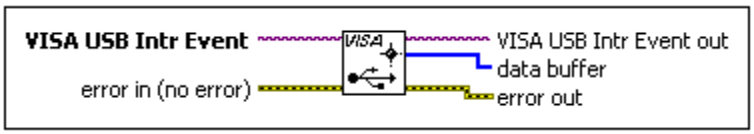

Figure 3.11 VISA Get USB Interrupt Data in Labview.

VISA USB Intr Event is a unique logical identifier to a VISA USB Interrupt Event.
Error in describes error conditions that occur before this VI or function runs.
VISA USB Intr Event out is a copy of the VISA USB Intr Event that is passed out of the VISA functions.

Data buffer is the buffer of USB interrupt data.
Error out contains error information. If **error in** indicates that an error occurred before this VI or function ran, **error out** contains the same error information. Otherwise, it describes the error status that this VI or function produces.
Error from the shortcut menu for more information about the error.

VISA Close Function:

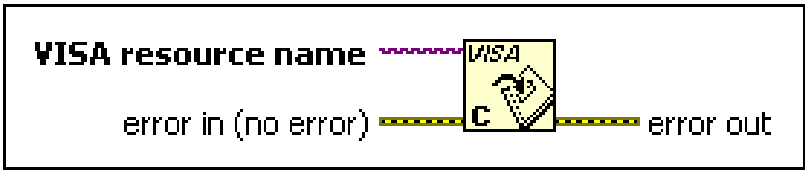

Fig 3.12 VISA Close Function in Labview.

VISA resource name specifies the resource to be opened. This control also specifies the session and class.
Error in describes error conditions that occur before this VI or function runs. The default is no error. If an error occurred before this VI or function runs, the VI or function passes the **error in** value to **error out**.
Error out contains error information. If **error in** indicates that an error occurred before this VI or function ran, **error out** contains the same error information.

Chapter 4

MESUREMENTS AND PERFORMANCES

4.1 Illumination distribution

Figure 7 shows three 3D surface plots that show the measured red (R), green (G), and blue (B) values of the 64 sensors from a single red, green, and blue LED, respectively. An LED is positioned to illuminate the center area of the sensor module and the distance from the LED to the sensor module is 25 cm. The highest optical intensity appears in the center area and the optical intensity decreases in the sensors near the border region. All sensors are set to the sensitivity level of 2. The color sensors convert the optical intensity (R, G, B) to voltage and the minimum measured voltage is 0 V when it is completely dark. The maximum measured voltage is 5 V when the received light is over the maximum received optical intensity. At that point, the 0 V is digitally encoded to 0, and 5 V is encoded to 255. The digital values are scaled from the received optical intensity. For the sensitivity level "zero", the irradiance responsivities, for the red color at 600 nm, is $S0_{Red}$ = 0.067 mV/ ($\mu W/cm^2$), for the green color, at 555 nm, the irradiance responsivities is $S0_{Green}$ = 0.063 mV/ ($\mu W/cm^2$), and for blue color, at 445 nm,, the irradiance responsivities is $S0_{blue}$ = 0.044 mV/ ($\mu W/cm^2$). From these values, we can estimate the maximum received optical intensity to measure, using TIAM2: $S0_{Red}$ Max = 5V / $S0_{Red}$ = 5000 / 0.067 = 74.62 (mW/cm^2) for red, $S0_{Green}$ Max = 5V / $S0_{Green}$ = 5000 / 0.063 = 79.37 (mW/cm^2) for green, and $S0_{blue}$ Max = 5V / $S0_{blue}$ = 5000 / 0.044 = 113.64 (mW/cm^2) for blue. These values are shown in Fig. 7. For the sensitivity level, "seven", the same calculation can be applied. The maximum received optical intensities for sensitivity level "seven" are 93.98 ($\mu W/cm^2$) for red, 99.8 ($\mu W/cm^2$) for green, and 143.27 ($\mu W/cm^2$) for blue.

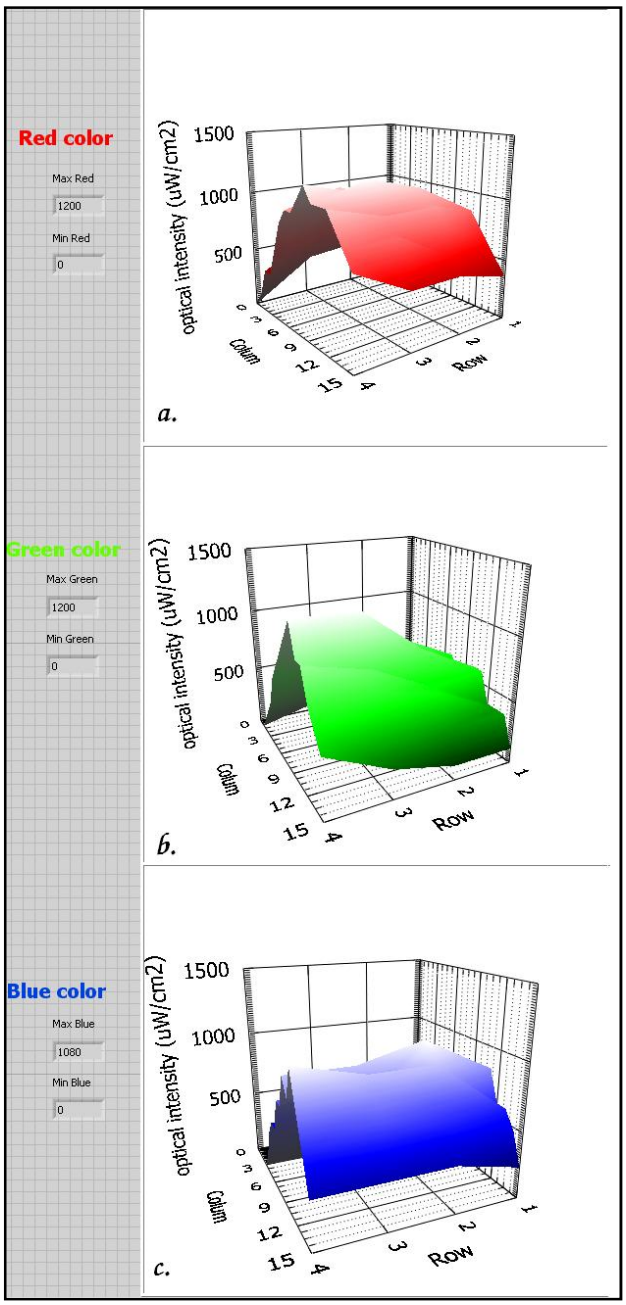

Fig4.1 Measured optical intensities for (a) red color, (b) green color, and (c) blue color.

The bottom surface means the geometrical measurement surface and the vertical axis means the scaled voltage, and, therefore, the relative measured intensity of each color and can be set to absolute values for measured intensity or illuminance with an exact adjustment process.

Fig. 8 shows the 1931 CIE chromaticity diagrams with the (*x*, *y*) coordinates for multiple sensors for R, G, B, and white LEDs. The chromaticity coordinates (*x*, *y*) correspond to its color. A measure of spread of *Y*, σ_Y, can be calculated as

$$\sigma_Y = \left(\frac{1}{N} \sum_{i,j} \left(Y_{i,j} - m_Y \right)^2 \right)^{1/2}, \tag{4}$$

where m_Y is the mean of *Y*, N is the number of *Y* values from color sensors, and $Y_{i,j}$ is the *Y* value of color sensor at (i, j) out of (16, 4). The uniformity of *Y* is defined in terms of its average value, m_Y, as

$$uniformity \ \ (\%) = \frac{\sigma_Y}{m_Y} \times 100 . \tag{5}$$

The uniformity of *Y* for an incandescent bulb is approximately 8.77 % with the distance of 50 cm to the sensor array module. Next, the color coordinates for LEDs of different colors are measured. The color coordinates are evenly distributed for each sensor. The measured color coordinates for a specific LED coincides with the color of the corresponding LED. As an example, the color coordinates for the white LED (Fig. 8(d)) are compared with the datasheet from the manufacturer. The measured *X* values are distributed around 0.37, while the measured *Y* values are distributed from 0.35 to 0.37. The datasheet provides the *X* values from 0.24 to 0.35, while the *Y* values are distributed from 0.24 to 0.35. As can be seen from this comparison, the developed measurement device provides the reliable color measurement for the sample white LED of the manufacturer. With precise adjustment on experimental conditions, the differences would be reduced.

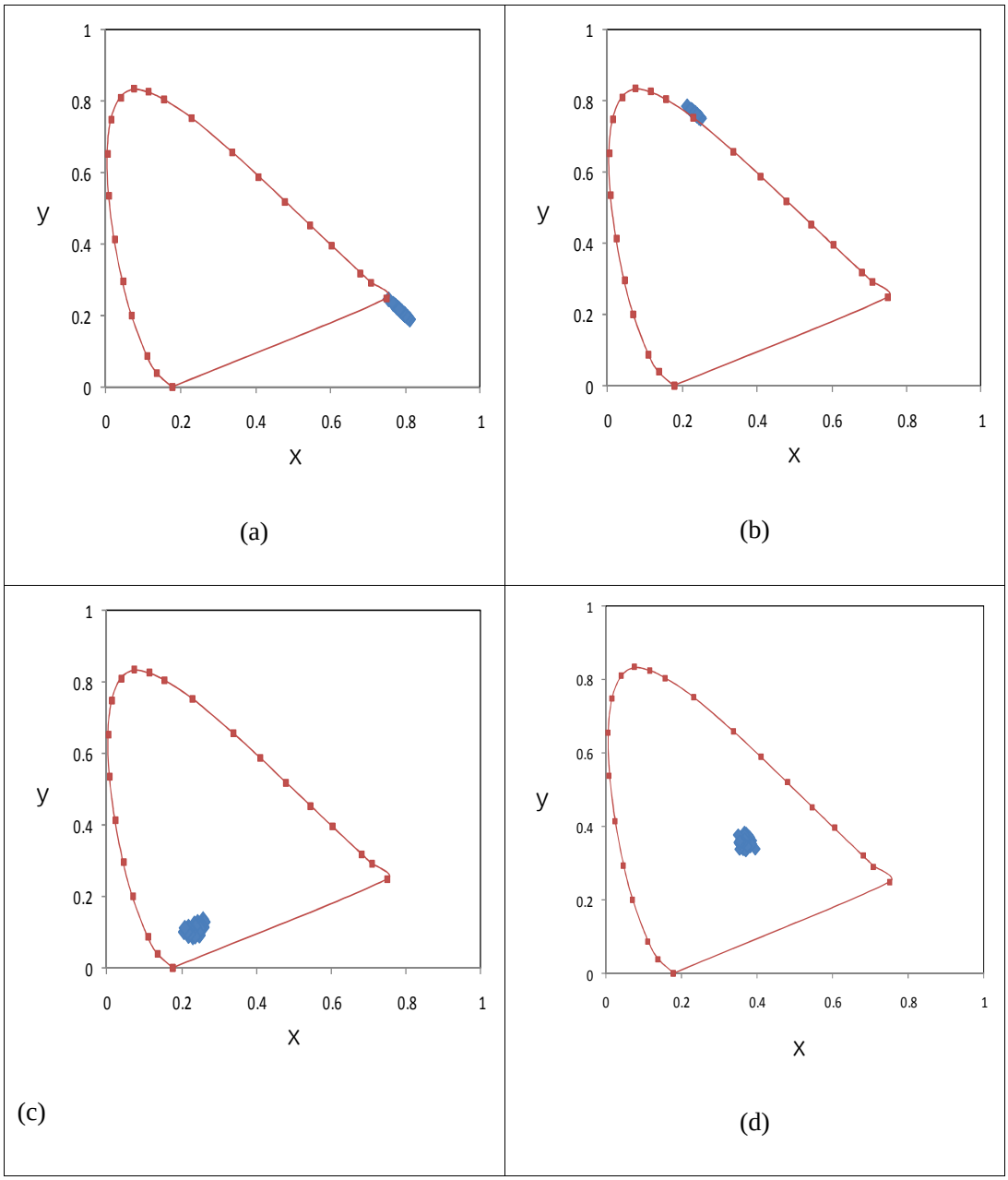

Fig 4.2 Measured 1931 CIE chromaticity diagrams for (a) a red LED, (b) a green LED, (c) a blue LED, and (d) a white LED. The red rectangles connected with the solid lines define the 1931 CIE chromaticity diagram. The blue overlapped diamonds denote the chromaticity coordinates from all color sensors.

4.2 Measurement sensitivity

Figure 9 shows the measured optical intensity for a red LED, with a different level of sensitivity, while maintaining the LED operating condition. It was tested with a single, commercial 1 W red-LED source at a distance of 20 cm.

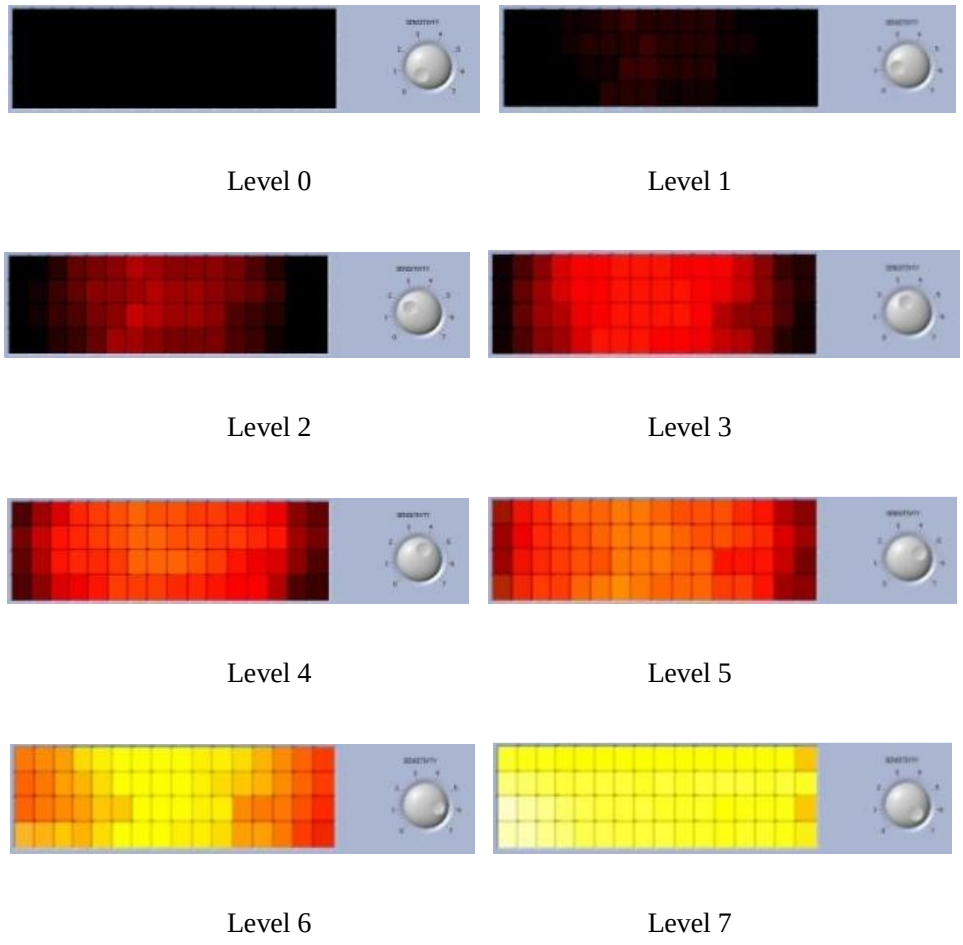

Fig 4.3 Optical intensity distribution for the increased sensitivity level with a red LED.

The sensitivity of the sensors is changed from the minimum value (Level 0) to the maximum value (Level 7). With Level 0, the sensor cannot detect the weak light. To detect the weak light,

the sensitivity level must be increased. If the sensitivity is too high, the color is expressed as yellow, for sensitivity Level 6 and sensitivity Level 7. The sensitivity level is changed digitally by programmable adjustment of transimpedance of the color sensor IC [15]. For a simple adjustment, with the known source-detector standard, the sensitivity of the sensor module can be adjusted by using the sensitivity knob on the front panel of the GUI in the PC.

The color sensor is a good candidate for a color measurement device because it includes the true color filters and an amplifier in a small package. Table 2 shows the electrical and optical characteristics of the color sensor [15]. From Table 2, the appropriate sensitivity level suitable for a specific application can be chosen.

Table 2 *The PD Sensitivity of the Used Color Sensor* [11]

Parameter	Symbol	Condition	Min.	Typ.	Max.	Unit
PD sensitivity of color ranges	S_{max}	λ_Z=445nm λ_Y=555nm λ_{Xk}=445nm λ_{Xl}=600nm	0.21 0.30 0.11 0.31	0.23 0.33 0.12 0.35	0.25 0.36 0.13 0.38	A/W

Figure 10 shows the photograph of the measurement device for a measurement. The control module is connected to the sensor array module using a 26-pin connector and to a PC through a USB connector. The sensor sensitivity is in Level 4. The light source is a 1-W red color LED. The optical intensities of red, green, and blue are shown on the PC screen. Since the measurement software is developed on the LabVIEW, we can stop the measurement procedure by clicking the stop button.

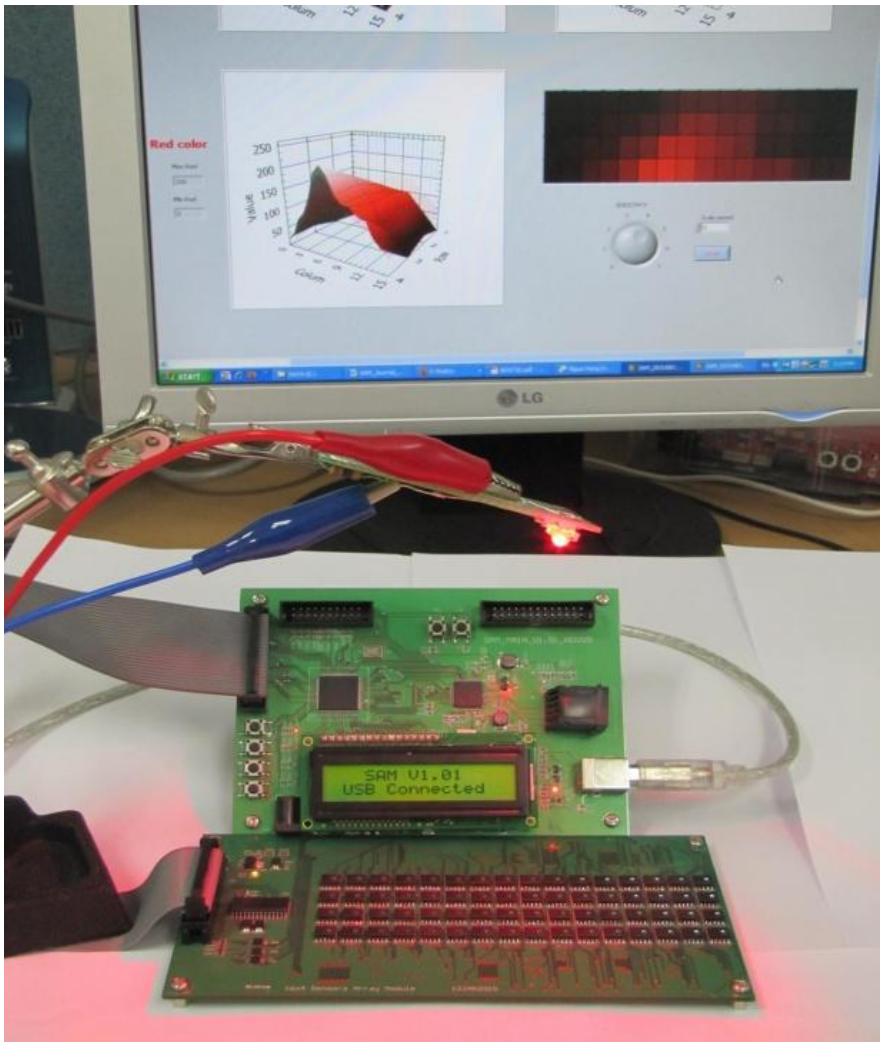

Fig 4.4 Setup using the developed measurement device. The sensor array module and the control module are shown.

4.3 ADC accuracy

We use a four channel, 12-bit sampling CMOS analog-to-digital converter (ADS 7824). The input range of the ADC is from –10V to +10V and provides a sufficient voltage range for converting the output of the color sensor. With this 12-bit ADC, the number of levels (NL) for each color is

$$NL = 2^{12} = 4096 \text{ (levels)}.$$

By generating the number of levels for three colors, we arrive at the number of color levels (NCL) as follows:

$$N_{C12} = (2^{12})^3 = 68{,}719{,}476{,}736 \text{ (colors)}.$$

We have 64 sensors with three colors (R, G, and B), and the number of total samples (NS) is

$$NS = 64 \text{ (sensors)} \times 3 \text{ (colors)} = 192 \text{ (samples)}.$$

The maximum sampling rate of ADS7824 is 40 kilo samples per second (ksps). Therefore, the minimum time required to convert the analog signal from the sensor module to the digital signal is

$$T_{CONV} = 192 \text{ (s)} / 40 \text{ (ksps)} = 4.8 \times 10^{-3} \text{ (s)} = 4.8 \text{ (ms)}.$$

The ARM-based microcontroller supports the USB 2.0 full speed interface. Therefore, we can transmit data to the PC at the maximum data rate of 12 Mbps. Since the 12-bit ADC is used, the total number of bits is

$$B_{TOTAL} = Ts \times 12 \text{ (bits/sample)} = 2304 \text{ (bits)}.$$

Therefore, the minimum time required to transmit data from the control module to the PC is

$$T_{TRAN} = 2304 \text{ (bits)} / 12 \text{ Mbps} = 192 \times 10^{-6} \text{ (s)} = 192 \text{ (us)}.$$

The minimum time required for conversion and transmission is

$$T_{TOTAL} = T_{CONV} + T_{TRAN} = 4.8 \text{ (ms)} + 192 \text{ (us)} = 4.992 \text{ (ms)}.$$

4.4 Measurement sensitivity Data processing speed

The ARM-based microcontroller (STR912FAW46X6), with a clock speed of 96 MHz, has enough processing speed to process and transmit data. In this development, we test the sensor array module, with the total time of T_{TOTAL} = 65 ms. 64 ms is required to convert data from the 64 sensors (1 ms for each sensor), and 1 ms is required for the transmission of data through the USB (~ 2.3 Mbps).

4.5 Compare with related work

There are several color measurement devices was developed. For example: “Imaging systems tackle color measurement” which was public in 2007 by Andrew Wilson. In this project, the author used three CCD sensor s and color filter to measure red, green and blue color.

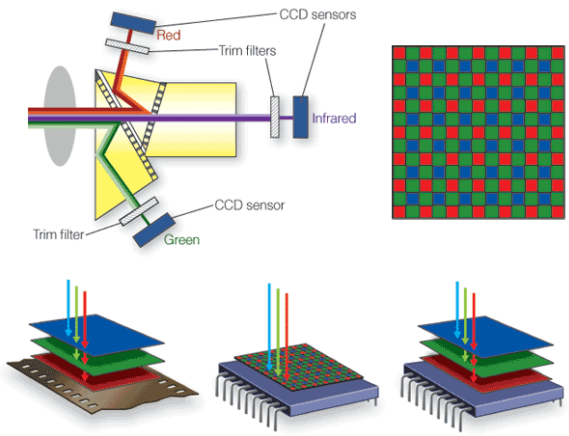

Fig 4.5 Imaging systems tackle color measurement

Other measurement device was public by Katherine Leo´n a. Its name is "Color measurement in L*a*b* units from RGB digital images". The author used a digital camera to take a picture of color sample. Computer analyzes, processes data and give out the result.

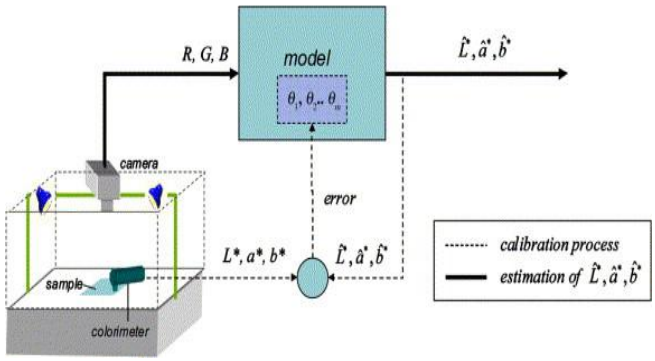

Fig 4.6 Color measurement in L*a*b* units from RGB digital images

Table 3. Compare with related work

Characteristics	Imaging systems tackle color measurement	Color measurement in L*a*b* units from RGB digital images	Illumination Measurement Device for Color Distribution Based on a CIE 1931 Sensor
Using	Difficult	Difficult	Easy
Speed	Slow	Slow	Fast
Shape	Big, cumbrous	Big, cumbrous	Small, sample
Cost price	Expensive	Expensive	Cheap

From this comparing, I believe this device can be used widely in the future.

Chapter 5

DISCUSSION

The processing of measurement data is performed using the ARM-based microcontroller. The measurement device can be upgraded by adding more RAM, ROM, and external flash memory to form an embedded illumination measurement device that works without a PC.
The measurement device can be developed as an embedded system with its own data display. The ARM-based microcontroller, running on a tiny OS, can collect, process, transmit, save, and retrieve the measurement data.

The Ethernet port can be used for exchanging measurement and control data with a PC via the Internet. The Internet-connected remote measurement device can be used to measure the illumination and color distributions in real-time inside or outside a building, for example, on the highway, the subway, etc. Furthermore, the measurement device can communicate with a GPS module to record the measurement data and measurement position during measurement.

Although 12-bit data for each color in this device is in compliance with the 36-bit color standard, only the eight most significant bits (MSBs) are used for each color to follow the 24-bit true color standard, as it is sufficient to display the color data on a PC screen. If the 12-bit ADC is upgraded to a 16-bit ADC, we can have 48-bit color and the device can measure and show 281.5 trillion colors [22].

We can use this device as a measurement device to characterize the indoor environment for developing an LED illumination system or an LED communication system. It will help illumination designers or interior designers to easily design an optimal illumination system by measuring the illumination at various positions.

Chapter 6

CONCLUSIONS

An easy-to-use, portable measurement device for illumination distribution has been developed. The device was designed with the purpose of providing a measurement tool useful for developing an LED illumination system and measuring indoor illumination. The array of CIE 1931 color sensors detects the illumination distribution and the CIE 1931 color coordinates. The measured data is transmitted to the PC through a USB interface and processed to draw graphs in the GUI.

The measurement of color coordinates from a white LED, using the measurement device, was tested by comparing the measured coordinates with the values in the data sheet from the manufacturer. The result shows a small difference. The development has provided a prototype measurement device for measuring the illumination distribution and the color coordinates.

References

1. E. F. Schubert, *Light-Emitting Diodes* (Cambridge University Press, Cambridge, 2003), Chapter 8.
2. A. Zukauskas, M. S. Shur, R. Caska, *Introduction to Solid-State Lighting*, (John Wiley & Sons, 2002) Chapter 7.
3. S. P. Ying, C.-W. Tang and B.-J. Huang, "Characterizing LEDs for mixture of colored LED light sources," presented at the 2006 EMAP International Conference on Electronic Materials and Packaging, Dec. 11-14, 2006.
4. S. Muthu, G. James, "Red, green and blue LED-Based white light source: implementation challenges and control design," Conference Record of the IAS Annual Meeting, (Salt Lake City, Oct. 2003), pp. 515-522.
5. J. J. Carr, *Sensors and circuit* (Prentice Hall, New Jersey, 1993).
6. Y. Tanaka, T. Komine, S. Haruyama, M. Nakagawa, "Indoor visible light data transmission system utilizing white LED lights," IEICE Trans. on Commun. **E86-B**, 2440-2454 (2003).
7. I. Moreno, M. Avedano-Alejo, R. I. Tzonchev, "Designing light-emitting diode arrays for uniform near-field irradiance," Appl. Opt. **45**, 2265-2272 (2006).
8. I. Moreno, C.-C. Sun, R. Ivanov, "Far-field condition for light-emitting diode arrays," Appl. Opt. **48**, 1190-1197 (2009).
9. A. J.-W. Whang, Y.-Y. Chen, Y.-T. Teng, "Designing uniform illumination systems by surface-tailored lens and configurations of LED arrays," Journal of Display Technol. **5**, 94-103 (2009).
10. J. H. Lee, W. Chang, D. Choi, "LED light coupler design for a ultra thin light guide," J. Opt. Soc. Korea, **11**, 113-117 (2007)
11. P. K. Yang, J. C. Chen, Y. H. Chuang, "Improvement on reflective color measurement using a tri-color LED by multi-point calibration," Opt. Commun. **272**, 320-324 (2007).

12. K. Liang, W. Li, H. R. Ren, X. L. Liu, W.J. Wang, R. Yang and D. J. Han, “Color measurement for RGB white LEDs in solid-state lighting using a BDJ photodetector,” Displays **30**, 107-113 (2009).
13. J.-B. Cheng, Q. Jiang, J.-J. Li, “Chromatic property measurement system for LED,” Proc. SPIE **5941**, 59411J (2005).
14. LiteMate (http://www.photoresearch.com).
15. Data Sheet of MTCS-TIAM2, “Integral True Color Sensor IC,” 2010.
16. CIE-1931 (http://en.wikipedia.org/wiki/CIE_1931_color_space).
17. C. DeCusatis (Editor), *Handbook of Applied Photometry* (AIP Press: New York, 1998).
18. ARM microcontroller (http://www.arm.com/products/processors/index.php**,** http://www.st.com/mcu/index.html).
19. Ethernet (http://www.altera.com/products/ip/iup/ethernet/m-mtip-10_100_ethermac.html).
20. USB (http:// www.beyondlogic.org/usbnutshell/usb-in-a-nutshell.pdf*)*.
21. J. Travis, *LabVIEW for Everyone: Graphical Programming Made Even Easier* (Prentice-Hall, Upper Saddle River, 1996) Chapter 11.
22. *Color Depth (*http://en.wikipedia.org/wiki/12_bit_color*)*.

ACKNOWLEDGEMENT

I would like to express my gratitude to my advisor, Prof. Lee Chung Ghiu, for his both insight and broad range of knowledge that he willingly shared with me during the research and writing of my dissertation. His advices are always very helpful, both academically and non-academically. It has been a great pleasure working with him.

I express my appreciation and indebtedness to my friends who co-worked in 2 years of my studying and helped me to adapt new environment: Choi Joon-choi, Jo Eul Byeol and Chang Hyung Joon.

I am extremely thankful to my parents and all my family for their love, support, teaching and encouragement in every moment of my life. From the bottom of my heart, I will ever always wish and pray for them.

Do Ky Son.

저작물 이용 허락서

학 과	전 자 공 학 과	학 번	20097785	과 정	석사
성 명	한글 도키손 한문 영문 DO KY SON				
주 소	광주시 동구 지산동 504-8				
연락처	e-mail : sondk89@gmail.com				
논문제목	한글: 컬러센서를 이용한 조명 및 컬러분포 측정장치 개발				
	영문: Development of an Illumination Measurement Device for Color Distribution Based on a CIE 1931 Sensor				

본인이 저작한 위의 저작물에 대하여 다음과 같은 조건 아래 조선대학교가 저작물을 이용할 수 있도록 허락하고 동의합니다.

- 다 음 -

1. 저작물의 DB 구축 및 인터넷을 포함한 정보통신망에의 공개를 위한 저작물의 복제, 기억장치에의 저장, 전송 등을 허락함
2. 위의 목적을 위하여 필요한 범위 내에서의 편집과 형식상의 변경을 허락함(다만, 저작물의 내용변경은 금지함)
3. 배포·전송된 저작물의 영리적 목적을 위한 복제, 저장, 전송 등은 금지함
4. 저작물에 대한 이용기간은 5 년으로 하고, 기간종료 3 개월 이내에 별도의 의사 표시가 없을 경우에는 저작물의 이용기간을 계속 연장함
5. 해당 저작물의 저작권을 타인에게 양도하거나 출판을 허락을 하였을 경우에는 1 개월 이내에 대학에 이를 통보함
6. 조선대학교는 저작물 이용의 허락 이후 해당 저작물로 인하여 발생하는 타인에 의한 권리 침해에 대하여 일체의 법적 책임을 지지 않음
7. 소속 대학의 협정기관에 저작물의 제공 및 인터넷 등 정보통신망을 이용한 저작물의 전송·출력을 허락함

동의여부 : 동의(0) 반대( )

2011 년 5 월

DO KY SON (인)

조선대학교 총장 귀하